Journal of Engineering Science and Technology
Special Issue on Development of Sustainability Systems - II, 193 - 205

EXPERIMENTAL INVESTIGATION ON THE THERMAL PERFORMANCE ENHANCEMENT OF FINNED THERMOELECTRIC COOLER POWERED BY SOLAR PHOTOVOLTAIC

NOOR A. A. TAHER[1,*], ALI A. F. AL-HAMADANI[1]

College of Engineering, Wasit University, Iraq
*Corresponding Author: ntaher@uowasit.edu.iq

Abstract

Thermoelectric cooling systems operating on the Peltier effect are an alternative to conventional systems. The greatest advantage of a thermoelectric cooling system is that it can be powered directly by solar photovoltaics. However, the main disadvantage of the thermoelectric cooling system is the low coefficient of performance, which increases with the improvement of the thermal performance. In this study, the thermal performance enhancement of the cold side of the thermoelectric cooler powered by integration with solar photovoltaic was assessed experimentally. Two experimental models of TEC with straight fins, namely Case-1, with 40 × 40 × 20 mm and 2 mm thickness, and Case-2, with 40 × 40 × 26 mm with 1 mm thickness. The experimental setup comprises of fan, blower, and thermoelectric coolers powered by a solar photovoltaic system as a DC source. Results show that the consumption current decreased from 5.1 A to 3.3 A when the cold side temperature increased by an average of 56%. While the input work dropped from 61.2 W to 39.6 W, the coefficient of performance rose from 0.0119 to 0.53. Additionally, using a 1 mm thickness enhanced the heat transfer rate from 0.339 to 10.52 W.

Keywords: Peltier effect, Solar energy, Straight fins, Thermoelectric cooler.

1. Introduction

The average global temperature has risen since the last century, so there is an urgent need for the use of cooling devices. It is estimated that air conditioning and cooling systems contribute about 15% of the global demand for electrical energy. The rapid depletion of non-renewable resources such as fossil fuels and their harmful emissions leads to the development of alternative solutions which invest renewable energy sources in cooling. Traditional vapour compression and vapour absorption refrigeration systems typically rely on fossil fuels for their operation, which ultimately generates a significant amount of CO_2 emissions [1, 2].

A thermoelectric cooler (TEC) is a cooling method that can replace Freon refrigerant and positively impact the greenhouse effect. A standard thermoelectric module comprises two ceramic substrates that serve as the base and electrical insulation for N-type and P-type Bismuth Telluride dice. The dice are thermally coupled in parallel between the ceramics and electrically connected in series. In addition, the ceramics serve as an insulator between any objects positioned against the module's cold side and any heat sink that needs to encounter the hot side [3, 4].

The thermoelectric generator (TEG) module presented a method to convert heat into electricity through the principle of the Seabeck effect, while TEC offered a method for converting the electrical energy into temperature difference [5]. The thermoelectric modules are convenient, light in weight, highly reliable, compact in size, noise-free (no moving part), and have no harmful emissions to the environment [6-9].

The TECs are used in various applications, such as cooling electronics, food, and humans. They disperse harmful heat in electronic parts like the central processing unit in a computer, graphics cards, and other parts [10]. TECs are also used to reduce the vehicle cabin temperatures and provide comfortable conditions for passengers [11]. Furthermore, TEGs are silent, scalable, and reliable, as they have no moving parts used by gadgets like tablets, Smartphones, and laptops. They are eco-friendly energy systems [12].

Due to the physical properties of TECs, their enhancements became the most frequent topic discussed. These physical properties are generated in the hot and cold sides of the thermoelectric cooler because of the Peltier effect, which works by applying a voltage difference between the two sides of the TEC, and as a result, a temperature difference will be generated [13, 14]. Different methods have been developed to measure the performance of the thermoelectric modules [15].

Vian's and Astrain developed a heat exchanger for the cold side of a thermoelectric cooler based on the principle of thermosyphon with phase change and capillary action. The device improved the thermal resistance by 37%, from 0.513 K/W of the finned heat sinks to 0.323 K/W. The experimental results proved that the COP of the thermoelectric cooler improved up to 32% (from 0.297 to 0.393) [16].

Heat sinks with different arrangements have been used to dissipate the heat from the TECs to improve their cooling performance [17]. Siahmargoi et al. [18] investigated the performance of a thermoelectric cooler using thermodynamic modelling and mathematical analyses and proposed a new correlation for performance evaluation of a thermoelectric cooler combined with two heatsinks (a heatsink on each side). The results showed that lowering the thermal resistance of

the hot side heatsink leads to the growth in the cooling power and the cold side temperature of the TEC. On the other hand, raising the thermal resistance of the cold side heatsink leads to dropping the cooling power of the system.

Although dispersing heat from the cold side of a thermoelectric cooler is important to improve its performance, there is little research on it. Most research is only concerned with the heat dispersing from the hot side. So, the idea in the present work is to use two models of straight fins on the cold side of a thermoelectric cooler powered by solar photovoltaic energy to enhance the heat transfer from the cold side of the PV-TEC and improve its thermal performance.

2. Experimental Methodology

The system consists of four essential components: solar panels, batteries, solar charge controller, and thermoelectric module, as shown in Fig. 1. Power is received from the solar panels, and then the solar charger regulates the process, and the battery stores the resulting current.

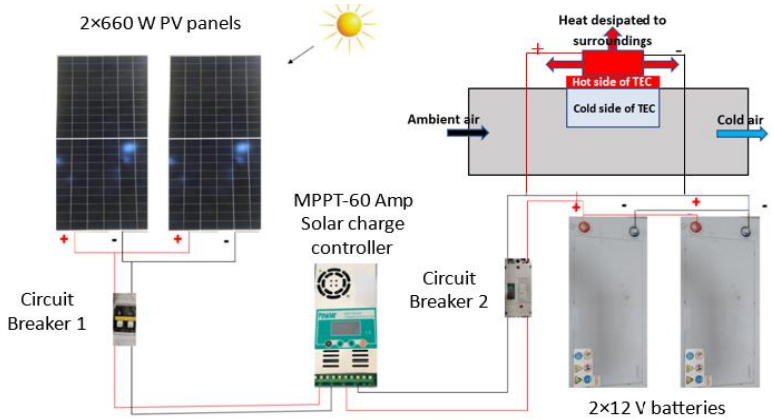

Fig. 1. The system description.

Two solar PV panels were used to convert the solar radiation to electrical energy and supply the power to the fan and blower in the cooling duct. Each panel was 660 W, and their dimensions were 2384 × 1303 × 35 mm. The cell type was Monocrystalline, and the type of manufacturer of the solar panels was MTS in Britain. The panels were connected in parallel, and their output was entered into the MPPT. The panels have a product warranty for 12 years. The features of the photovoltaic panels are shown in Table 1, and the PV panels are shown in Fig. 2.

Fig. 2. The photovoltaic panel.

Table 1. The features of the PV panel.

Feature	Value
Cells type	**Monocrystalline**
Maximum Power (Pmax)	660 W
Open-circuit Voltage (Voc)	45.6 V
Short-circuit Current (Isc)	18.44 A
Maximum Power Voltage (Vmp)	37.9 V
Maximum Power Current (I mp)	17.42 A
Module Efficiency	21.25 %
No. of Cells	132 (2×66)

The MPPT solar charge controller, with specifications shown in Table 2, is more efficient and low-cost, was used to adapt its input voltage to maximize power harvesting from the solar panels and then transform this power to supply the varying voltage requirement of the batteries. Therefore, it separates the voltages of the panels and the batteries in such a way that the MPPT charge controller has 12V batteries connected to one side and 40 V panels connected in parallel to the other. The MPPT calculates the PV voltage and output power and the battery state of charge and manages the charging of the batteries.

Table 1. The features of the MPPT.

Feature	Value
MPPT current	60 A
Absorption voltage for GEL battery 12 V	14.4 V
Limited current protection	61 A
Max efficiency	> 98.1 %
Size	214 × 115 × 50 mm

The system used two GEL batteries to store the electrical energy produced by the PV panels. The two batteries were connected in parallel, and the output from them was connected to a circuit breaker. After that, the output from the circuit breaker was interconnected to the MPPT. The thermoelectric cooler (TEC) 6A had input power from the photovoltaic panels that charged the batteries, and its features are shown in Table 3.

Table 3. The features of TEC.

Characteristics of TEC	Values (unit)
Model number	TEC1-12706
Operating voltage	12 V
Maximum current, Imax	6 A
Maximum voltage, Vmax	15.4 V
Maximum power	92 W
Maximum temperature	138 ºC
Power cord	200 mm
Dimensions	40 × 40 × 3.4 mm

The TEC was fixed in a wooden duct of 240 × 120 × 60 mm covered with an aluminium sheet of 0.5 mm thickness. The hot side of the thermoelectric cooler is

connected to the sunflower heat sink on the upper surface of the duct, and they are shaped as a heat sink which functions as a dissipator, taking in heat from the hot side of the Peltier module. Additionally, a 12 V fan is connected to the heat sink to lower the temperature on the hot side, and a DC power source (solar photovoltaic system). The ambient air flowed through the cooling duct by forced convection using a blower positioned in the duct inlet. The cold side of the TEC is located on the inner surface of the cooling duct. Two types of heat sinks were tested with different designs, as shown in Fig. 3.

a. Case-1: The cold side of the TEC was connected to straight fins 40 × 40 × 20 mm, and its thickness was 2 mm.

b. Case-2: The cold side of the TEC was connected to straight fins 40 × 40 × 26 mm, and its thickness was 1 mm.

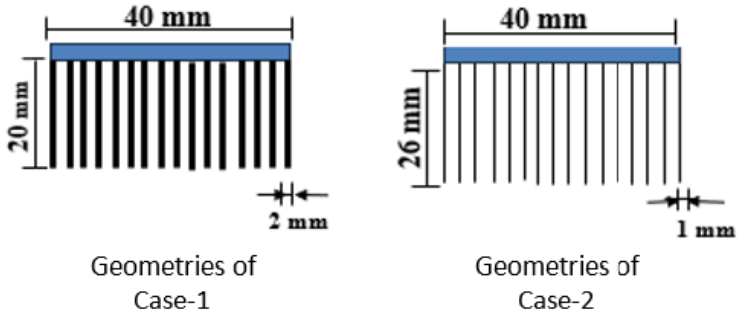

Fig. 3. The geometries of straight fins design of the cold side.

The ambient air enters the cooling duct by the blower and the TEC used to cool the duct. The cold side fins exchange heat with the flowing air inside the duct. The hot side of the TEC dissipates the heat from the cold side by forced convection from the body of the TEC to the surroundings. The experimental arrangement of this cooling criteria is shown in Fig. 4.

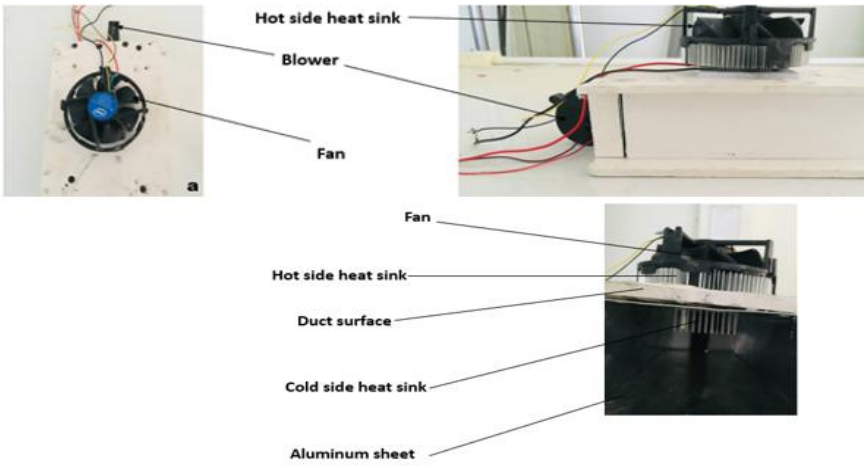

Fig. 4. The experimental arrangement of the cooling duct.

Solar irradiation was measured using a solar power meter, and temperatures were measured using a data acquisition system (Arduino MEGA 2560, MAX6675 thermocouple sensor module, and thermocouples). The measuring instruments and their accuracies are presented in Table 4.

Table 4. The errors and actuary of the instruments' measurement devices.

Measurement device	Errors and accuracy
Solar power meter	±10 W/m^2
Clamp Multimeter	±0.003 - 1 A
Thermocouple	±0.5 - ±1% ^{o}C
Hot wire anemometer	±0.1 - ±3% m/s

The adopted procedure to perform the research is presented in Fig. 5 as a flowchart.

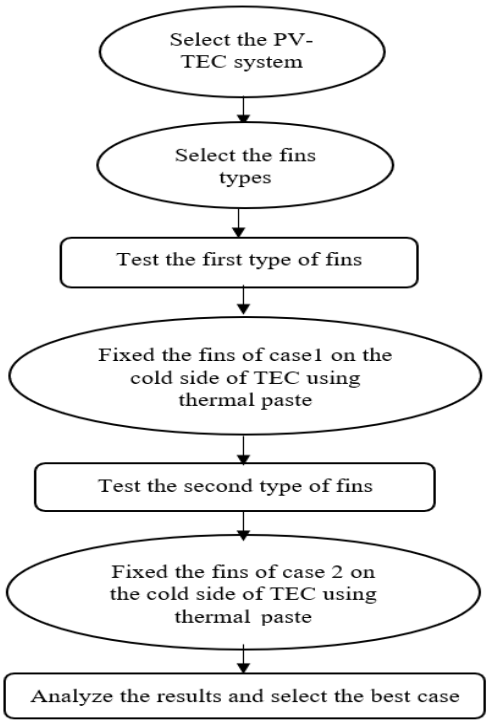

Fig. 5. The methodology flow chart.

3. Data Reduction

The amount of heat to be removed or absorbed by the cold side of the TEC [19]

$$Q_c = \dot{m} \times C_p \times \Delta T \quad (1)$$

where ΔT is the temperature difference between ambient temperature and cold air temperature measured at the exit from the cooling duct, the mass flow rate is predicted by Eq. (4).

$$\dot{m} = \rho \times u \times A_c \quad (2)$$

where A_c is the Cross-section area of the cooling duct.

The input work, W_{in} to the TEC, is the power generated by the PV predicted by Eq. (3).

$$W_{in} = \mathrm{I} \times \mathrm{V} \tag{3}$$

I and *V* are the current and voltage of the PV system.

Then, the coefficient of performance (COP) could be determined by Eq. (4)

$$COP = \frac{Q_c}{W_{in}} \tag{4}$$

The heat transfer rate

$$Q = h \times A_s \times (Ts - T\infty) \tag{5}$$

where T_s is the surface temperature, and T_∞ is the ambient temperature.

$$Re = \frac{\rho\, u\, x}{\mu} \tag{6}$$

$$P_r = \frac{\mu C_p}{k} \tag{7}$$

$$x = \frac{2ab}{a+b} \tag{8}$$

For fully developed turbulent flow in smooth tubes with moderate temperature difference, Nu could be predicted using Eq. (9), and then the convective heat transfer could be estimated using Eq. (10). [20]

$$Nu_d = 0.023 \times Re_d^{0.8} \times Pr^n \tag{9}$$

$$n = \begin{cases} 0.4 & for\ heating\ of\ the\ fluid \\ 0.3 & for\ cooling\ of\ the\ fluid \end{cases}$$

$$h = \frac{Nu \times k}{x} \tag{10}$$

$$m = \sqrt{\frac{h \times P}{k \times A}} \tag{11}$$

$$q_{fin} = \sqrt{\mathrm{h} \times \mathrm{P} \times \mathrm{k} \times \mathrm{A}}\, \theta_\circ \tanh ml \tag{12}$$

The ambient air enters the cooling duct by the blower and the TEC used to cool the duct. The cold side fins dissipated the heat from the cold side of TEC and exchanged heat with the flowing air inside the duct. The fan and hot side fins dissipated the hot air generated by the hot side of the TEC.

4. Results and Discussion

In this part, all the results of the study are presented. Different parameters are studied to examine the performance of the TEC.

4.1. Experimental boundary conditions

Figure 6 shows the variation of solar radiation with time. For case-1, the solar radiation descended from 791 to 685 W/m^2. For case-2, the solar radiation increased

from 498 to 611 W/m^2, with increasing the time from 11:30 AM to 1:00 PM. After that, Ir started to drop to 595 W/m^2 at 1:30 PM.

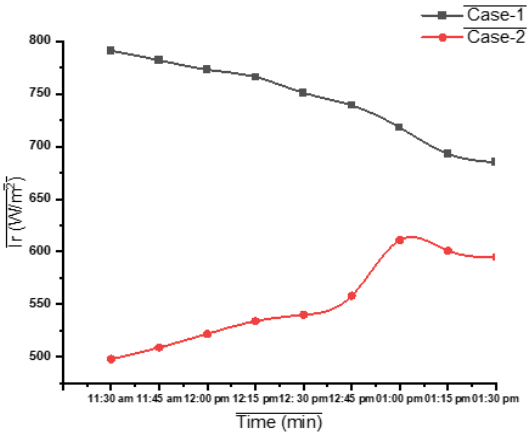

Fig. 6. Variation of solar radiation vs. time of experiment.

4.2. The effect of fins models on the cold side temperature

Figure 7 shows the reduction of the cold side temperature of the two experimented cases over two hours of running. The results indicate that the cold side temperature decreased by about 36% in case-1. However, the cold side temperature decreased by about 56% in case-2. This difference means that the design of the fins according to cas-2 is more efficient than case-1. This is due to the lower thickness of the plate fins in case-2 and the larger area, as the fin length is 26 mm, while for case-1, the fin length is 20 mm.

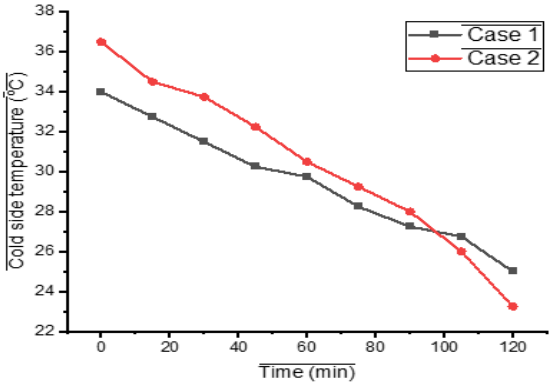

Fig. 7. Variation of the cold side temperature over time.

4.3. Effect of supply current

Figure 8 shows the behaviour of the cold side temperature when the supplied current varied for the two models of fins, case 1 and case 2. In case-1, the current started at 5.1 A and dropped to 3.4 A, while in case-2, the consumption current began at 5.1 A and decreased to 3.3 A. The drop in the cold side temperature for

case 2 is higher than that in case 1. This reduction in current is due to the lowering in the cold side temperature which leads to a decrease in the applied load. The temperature drop in case 1 is from 34 °C to 24.5 °C, while for case 2 is from 36.6 °C to 23.2 °C.

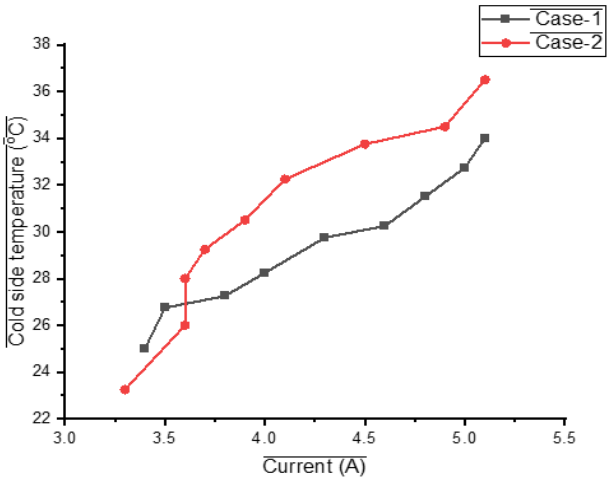

Fig. 8. Variation of fins models vs. current.

4.4. Effect of fins models on COP

Figure 9 shows the relation between input work and COP under the effect of fins models. In case-1, the COP increased steadily from 0.012 to 0.44, and the input work decreased from 61.2 to 40.8 W. While in case-2, the COP grew from 0.0119 to 0.53, and the input work dropped from 61.2 to 39.6 W. The increase in COP was from Eq. (4) (the COP inverse relationship with the input work). The input work reduction is due to the reduced consumption of voltage and current by the TEC as a result of the reduced cold side temperature.

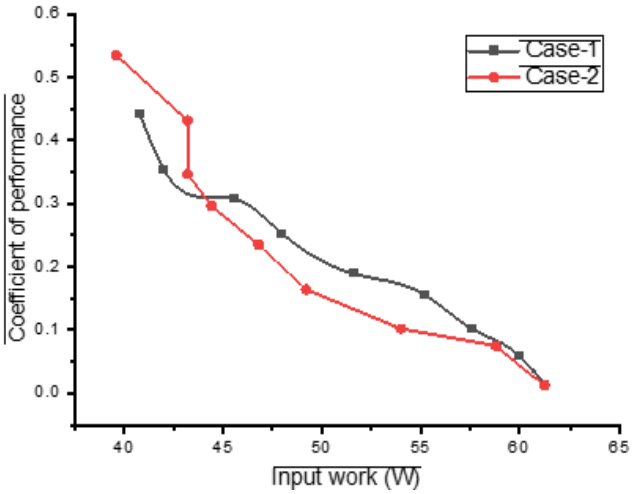

Fig. 9. Variation COP with change in the input work to TEC.

Figure 10 shows the relation between temperature difference and COP for different models of fins. In case-1, the COP increased regularly from 0.012 to 0.44, with growing the temperature difference, which is the difference between ambient and cold side temperatures from 0.5 to 11.5 °C. In case-2, the COP raised from 0.0119 to 0.53, with increasing the temperature difference from 0.5 to 14.5 oC. The increase is due to the rise in the temperature difference, according to Eq. (1).

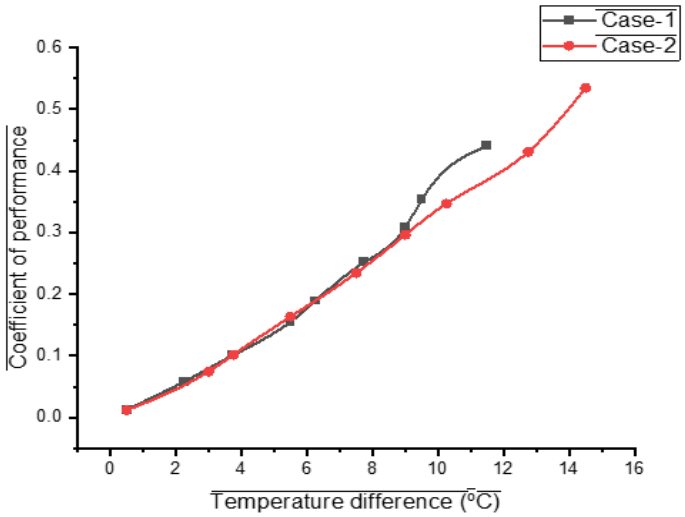

Fig. 10. Variation of COP with changes in temperature difference of TEC.

5. Conclusions

In the present work, an experimental study was done to enhance the thermal performance of the cold side of a thermoelectric cooler powered by solar energy. Case-2 was better than case-1 and the following has been concluded.

- The cold side temperature decreased by about 56% compared with Case-1.
- The consumption current decreased from 5.1 A to 3.3 A under steady-state conditions.
- The input work needed to operate the system was dropped from 61.2 W to 39.6 W.
- The difference between ambient and cold side temperatures in Case-2 increased from 0.5 °C to 14.5 °C.
- The COP which is the most important factor for thermoelectric performance parameter, raised from 0.0119 to 0.53 in Case-2.

For future works in this line, it is recommended to perform a simulation using COMSOL software to extend and ranges of the inputs and also to investigate and compare more designs. Using phase-change material to enhance the thermal performance of a thermoelectric cooler.

Acknowledgement

I would like to express my thanks to ***the faculty and administrative staff*** in the College of Engineering/Wasit University for their cooperation and professional treatment.

Nomenclatures

A_c	The cross-section area of the cooling duct, m^2
C_p	Specific heat of the fluid, kJ/kg·K
h	Convection heat transfer coefficient, $W/m^2 \cdot K$
I	The current of the TEC, Amp
k	Thermal conductivity, W/m·K
$\dot{m}$	The mass flow rate of the fluid, kg/s
$Q_{conv.}$	Convection heat transfer rate, W
T_c	Cold side temperature, K, ^oC
T_h	Hot side temperature, K, ^oC
T_{amb}	Ambient temperature, K, ^oC
T_{out}	Outlet temperature, K, ^oC
u	Air velocity, m/s
V	The voltage of the TEC, V
W_{in}	Input work, J

Greek Symbols

μ	Dynamic viscosity, Pa.s
ν	Kinematic viscosity, m^2/s
ρ	Fluid density, kg/m^3

Abbreviations

AC	Air Conditioning
Al	Aluminium
COP	Coefficient of Performance
TDC	Temperature difference between ambient temperature and cold side temperature
DC	Direct current
MPPT	Maximum Power Point tracker
Nu	Nusselt number
Pr	Prandtl number
PV	Photovoltaic
PV-TEC	Photovoltaic Thermoelectric coder
Re	Reynolds number
TEC	Thermoelectric cooler
TEG	Thermoelectric generator

References

1. Win, S.L.Y.; Chiang, Y.-C.; Huang, T.-L.; and Lai, C.-M. (2024). Thermoelectric generator applications in buildings: A review. *Sustainability*, 16(17), 7585.
2. Fathima, A.B.; Raj, A.R.; Mohan, C.J.; Rodriguez, E.S.; and Daniel, J.J. (2019). Solar powered automatic cabin cooling system. *Global Research and Development Journal for Engineering*, 4(13), 252-269.
3. Sakthivel, C.; Jethose, V.; Selvakumar, K.; Raja, K.; and Kumar, P.D. (2018). A new topology power generation system with MPPT. *Global Research and Development Journal for Engineering*, 4, 293-300.

4. Cai, Y.; Liu, D.; Yang, J.-J.; Wang, Y.; and Zhao, F.-Y. (2017). Optimization of thermoelectric cooling system for application in CPU cooler. *Energy Procedia*, 105, 1644-1650.
5. Lim, C.C.; Al-Kayiem, H.H.; and Sing, C.Y. (2014). Portable thermoelectric power generator coupled with phase change material. *MATEC Web of Conferences*, 13, 02028.
6. Al-Hamadani, A.A.F.; and Ali Taher, N.A.-H. (2024). Thermoelectric cooling system for vehicle cabin during parking powered by solar photovoltaic energy. *Journal of Advanced Research in Fluid Mechanics and Thermal Sciences*, 121(1), 17-26.
7. Srivastava, R.S.; Kumar, A.; Thakur, H.; and Vaish, R. (2022). Solar assisted thermoelectric cooling/heating system for vehicle cabin during parking: A numerical study. *Renewable Energy*, 181, 384-403.
8. Omkar, S.; Yogesh, N.; Gorakhnath, G.; and Omkar, G., (2020). Air conditioning system in car using thermoelectric effect. *International Journal of Engineering Research & Technology* (*IJERT*), 9(6), 374-377.
9. K. Shilpa, M.; Abdul Raheman, M.; Aabid, A.; Baig, M.; K. Veeresha, R.; and Kudva, N. (2023). A Systematic review of thermoelectric Peltier devices: Applications and limitations. *Fluid Dynamics and Materials Processing*, 19(1), 187-206.
10. Mitofsky, A.M. (2018). *Direct energy conversion*. CreateSpace Independent Publishing Platform.
11. T. Taher, N.A.-A.; and Al- Hamadani, Ali A.F. (2024). Systematic review: How to reduce the car cabin temperature using solar energy? *Wasit Journal of Engineering Sciences*, 2(12), 15-32.
12. Mamur, H.; Dilmaç, Ö.F.; Begum, J.; and Bhuiyan, M.R.A. (2021). Thermoelectric generators act as renewable energy sources. *Cleaner Materials*, 2,100030.
13. Wiriyasart, S.; Suksusron, P.; Hommalee, C.; Siricharoenpanich, A.; and Naphon, P. (2021). Heat transfer enhancement of thermoelectric cooling module with nanofluid and ferrofluid as base fluids. *Case Studies in Thermal Engineering*, 24, 100877.
14. Cai, Y.; Wang, Y.; Liu, D.; and Zhao, F.-Y. (2019). Thermoelectric cooling technology applied in the field of electronic devices: Updated review on the parametric investigations and model developments. *Applied Thermal Engineering*, 148, 238-255.
15. Riyadi, T.W.B.; Utomo, B.R.; Effendy, M.; Wijayanta, A.T.; and Al-Kayiem, H.H. (2022). Effect of thermal cycling with various heating rates on the performance of thermoelectric modules. *International Journal of Thermal Sciences*, 178, 107601.
16. Vián, J.G.; and Astrain, D. (2008). Development of a heat exchanger for the cold side of a thermoelectric module. *Applied Thermal Engineering*, 28(11-12), 1514-1521.
17. Naphon, P.; Wiriyasart, S.; and Hommalee, C. (2019). Experimental and numerical study on thermoelectric liquid cooling module performance with different heat sink configurations. *Heat and Mass Transfer*, 55(9), 2445-2454.

18. Siahmargoi, M.; Rahbar, N.; Kargarsharifabad, H.; Sadati, S.E.; and Asadi, A. (2019). An experimental study on the performance evaluation and thermodynamic modeling of a thermoelectric cooler combined with two heat sinks. *Scientific Reports*, 9(1), 20336.
19. Raut, M.S.; and Walke, P.V. (2012). Thermoelectric air cooling for cars. *International Journal of Engineering Science and Technology* (*IJEST*), 4(5), 2381-2394.
20. Al-Kayiem, H.H.; and El-Rahman, M.F. (2011). Ribbed double pipe heat exchanger: Analytical analysis. *Journal of Engineering Science and Technology* (*JESTEC*), 6(1), 39-49.